Journal of Alloys and Compounds, 203 (1994) 165–168
JALCOM 865

Structural phase transformation and shape memory effect in ZrRh and ZrIr

Elena L. Semenova
I.N. Frantsevich Institute for Problems of Material Science, Academy of Science of Ukraine, Kiev (Ukraine)

Yu. V. Kudryavtsev
Institute of Metal Physics, Academy of Science of Ukraine, Kiev (Ukraine)

(Received June 17, 1993)

Abstract

Crystal structure investigations of the ZrRh and ZrIr compounds have shown the occurrence of a B19′-type phase at room temperatures, a B2-type phase at 670 and 1050 °C respectively and a b.c.c. phase for ZrRh in the temperature interval from 1455 °C to the melting point. The shape memory effect was observed for ZrRh and can be expected too for ZrIr in view of the very similar transformation characteristics of ZrRh and ZrIr.

1. Introduction

While investigating the phase equilibria in the Zr–Rh and Zr–Ir binary systems, we have discovered that the equiatomic phases of these systems undergo a transformation similar to that in the TiNi compound [1]. The latter is interesting because of its thermomechanical properties. X-ray analysis of the ZrRh and ZrIr alloys at room temperature was carried out in refs. 2 and 3. Dwight found that ZrIr revealed extremely complex patterns from which he could not identify its structure [2]. Raman and Schubert discovered the ZrRh and ZrIr phases to be isostructural [3]. Wang, by means of the single-crystal X-ray diffraction method, established the existence of a transformation in ZrRh at 380 °C on cooling [4] which was similar to that found in TiNi. Jorda *et al.* [5] interpreted the crystal structure of the ZrRh phase as orthorhombical (type FeB) but expressed doubts about the correctness of this structure determination.

The purpose of this paper is to report our experimental data from a study of the structural phase transformation and shape memory effect in the equiatomic ZrRh and ZrIr alloys.

2. Experimental procedure

The starting materials for synthesis of the alloys were rhodium powder, iridium rod and iodized zirconium, all of a nominal purity of 99.9 wt.%. The rhodium powder was annealed in vacuum and then, like the iridium rod, remelted in order to avoid further sputtering during alloying. The alloys were melted under an atmosphere of purified argon gas in an arc furnace with a non-consumable electrode on a water-cooled copper bottom. Since ZrRh is structurally related to TiNi, the TiNi alloy was also prepared from iodized titanium (99.9 wt.%) and nickel (99.99 wt.%). The weight losses on melting were small, so nominal compositions are reported. The accuracy of the nominal compositions was estimated to be ±0.25 at.%. The investigation of the alloys was carried out using metallographic, differential thermal and electrical resistivity analyses [1]. The crystal structure was investigated by the X-ray diffraction method using high temperature diffraction experiments [6]. The thermomechanical tests were performed by three-point bending [7].

3. Results and discussion

The ZrRh and ZrIr phases crystallize from the melt with melting points of 1890 and 2050 °C respectively and have homogeneity ranges on the platinum metal side with maximum intervals of about 10 at.% Rh and 3 at.% Ir respectively (Fig. 1) [1]. On cooling, the ZrRh and ZrIr phases undergo a transformation. Typical examples of the striped microstructures observed are shown in Fig. 2.

By the method of thermal analysis, two solid transformations at 610 and 1455 °C were found to exist for

SSDI 0925-8388(93)00865-V

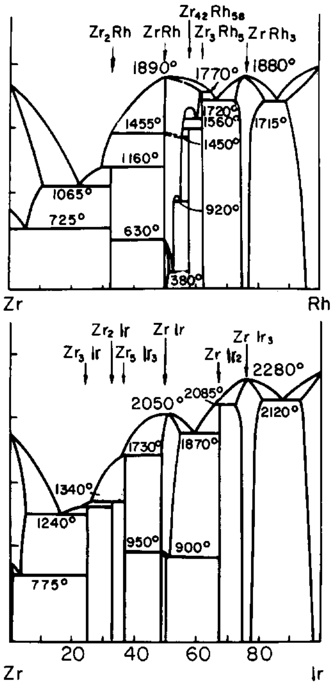

Fig. 1. Zr–Rh and Zr–Ir phase diagrams.

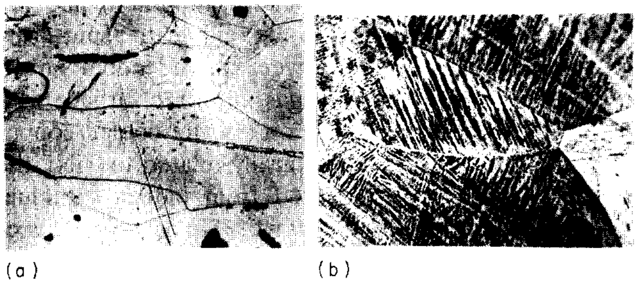

Fig. 2. Microstructures of alloys with (a) 52 at.% Rh, quenched from 1650 °C (δ phase), and (b) 52 at.% Ir, annealed at 1700 °C (striped δ' phase) (magnification, ×200).

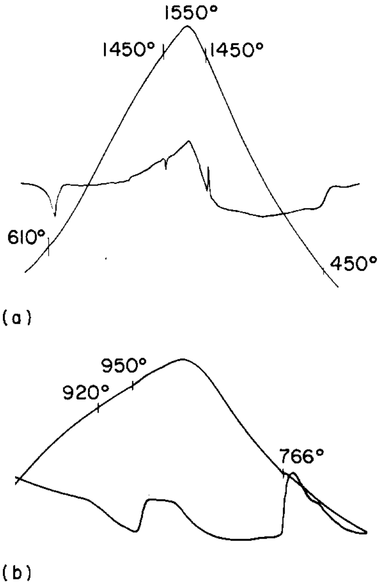

Fig. 3. Differential thermal analysis data on solid state transformation in (a) ZrRh and (b) ZrIr alloys: (a) 610↑(450↓) °C, δ'⇆δ''; 1450 °C, δ⇆δ'; (b) 950↑(766↓) °C, δ'⇆δ''.

TABLE 1. X-Ray data for the high temperature forms of ZrIr (1050 °C) and ZrRh (670 °C)

hkl	ZrIr		ZrRh	
	I/I_0	d_{obs} (Å)	I/I_0	d_{obs} (Å)
001	0.60	3.32	0.02	3.30
011	1.00	2.35	0.41	2.33
002	0.79	1.66	1.00	1.65
112	0.18	1.36	0.06	1.35
022	0.07	1.17	0.02	1.17
013	0.20	1.05	0.11	1.04
321	0.13	0.88	0.06	0.88
400	0.10	0.83	0.12	0.82

ZrRh and one solid transformation at about 920 °C for ZrIr on heating (Fig. 3). Analogously to the known equiatomic binary systems of transition metals and according to ref. 4, it was assumed that the B2 phase existed above room temperature. The diffractograms of ZrIr at 800, 950 and 1050 °C on heating and of ZrRh at 450, 600 and 670 °C on heating and at 380 and 350 °C on cooling were obtained. The X-ray diffractograms of ZrRh and ZrIr at 670 and 1050 °C respectively were indexed unambiguously in the cubic B2-type crystal structure with the lattice parameters $a = 3.295$ Å (ZrRh) and $a = 3.318$ Å (ZrIr) (Table 1). Only the superstructure line (100) was observed. This structure for the ZrRh phase persisted on cooling to 380 °C, but at 350 °C the diffraction pattern changed sharply. The intensity of the (110) reflection decreased and an additional reflection appeared. Temperature hysteresis was observed: on heating to 450 °C, the B2 phase was still not present. The TiNi, ZrRh and ZrIr fragments of X-ray diffractograms obtained above the transformation temperatures and at room temperature are shown in Fig. 4. The TiNi diffractogram at 210 °C was indexed in the cubic B2-type crystal structure ($a = 3.015$ Å) and that at room temperature in the monoclinic B19'-type structure ($a = 2.88$ Å, $b = 4.68$ Å, $c = 4.14$ Å, $\beta = 97.2°$), which is in good agreement with ref 8.

The X-ray diffractograms of ZrRh and ZrIr at room temperature before and after heating were identical, with low intensities and broadened reflections at angles above 30° (about 0.5°–2° at half-height). Comparison of these with the TiNi diffractograms made it possible to index them in the monoclinic B19' crystal structure with the lattice parameters $a = 3.31$ Å, $b = 4.32$ Å, $c = 5.31$ Å and $\beta = 100.4°$ for ZrRh and $a = 3.33$ Å, $b = 4.38$ Å, $c = 5.35$ Å and $\beta = 99.0°$ for ZrIr. The results of in-

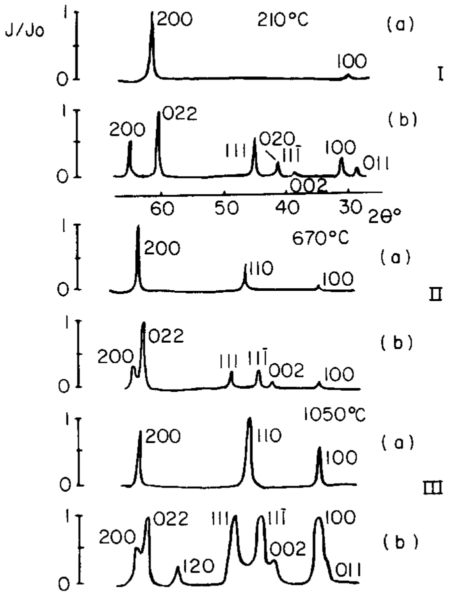

Fig. 4. TiNi (I), ZrRh (II) and ZrIr (III) fragments of X-ray diffractograms at room (a) and high (b) temperatures.

TABLE 2. X-Ray data for the room temperature forms of ZrIr and ZrRh

hkl	ZrIr		ZrRh	
	d_{calc} (Å)	d_{obs} (Å)	d_{calc} (Å)	d_{obs} (Å)
011	3.36	3.36	–	–
100	3.28	3.28	3.26	3.27
002	2.63	2.63	2.61	2.61
11$\bar{1}$	2.49	2.48	2.47	2.46
111	2.23	2.22	2.20	2.19
120	1.82	1.83	–	–
022	1.68	1.68	1.67	1.67
200	1.64	1.64	1.63	1.63
201	1.50	1.50	–	–
030	1.46	1.46	–	–
211	1.42	1.42	–	–
220	1.31	1.32	–	–

dexation and the comparison with experimental data are given in Table 2.

It should be noted that the *b*, *c* and doubled *a* parameters calculated by us for the ZrRh compound are close to the values $a = 6.63$ Å, $b = 4.41$ Å and $c = 5.39$ Å for the orthorhombic FeB-type structure [5]. Nevertheless, our attempt to index the ZrRh diffractogram in the orthorhombic structure failed.

The thermal curves of two-phase $Zr_2Rh + ZrRh$ alloys (Figs. 1 and 3) revealed a transformation of the δ' phase on cooling to a temperature of 630 °C. The increase in the transformation temperature for these alloys as compared with that for the equiatomic alloy points to the existence of some homogeneity range of ZrRh on the zirconium side. In alloys containing more than 50 at.% Rh the transformation temperature decreased. According to the differential thermal analysis data, the temperature of the other transformation found in the alloy with 50 at.% Rh at 1455 °C remained the same in the range L + ZrRh and changed slightly in the ZrRh homogeneity range. The maximal thermal effect due to this transformation corresponds to the equiatomic composition. This means that this transformation can be attributed to the equiatomic ZrRh phase. As can be seen from the metallographic and X-ray analyses of the alloy with 52 at.% Rh quenched from 1650 °C (Fig. 2), it contains a single phase with the cubic structure. Assuming both the known properties of equiatomic phases with cubic structure to increase their stability at elevated temperatures and the occurrence of a B2-type structure at 670 °C, the thermal effect at 1455 °C can be attributed to the ordering of the b.c.c. phase to a B2-type phase. Thus crystal structure determinations of ZrRh have shown that this compound crystallizes in the b.c.c. structure, transforms to a closely related B2-type structure at 1455 °C and transforms to an orthorhombic B19′-type structure at 350 °C. The structural transformations of the δ phase on cooling can be written as

$$\delta(\text{b.c.c.}) \longrightarrow \delta'(\text{B2}) \longrightarrow \delta''(\text{B19}')$$

The transformation in ZrIr alloys containing less than 50 at.% Ir took place at 950 °C. The transformation in the equiatomic alloy occurred in the temperature interval 920–950 °C. This fact indicates the existence of a small homogeneity range at these temperatures. The other transformation found in the ZrRh alloys was not observed in the case of ZrIr. It can be seen that the Zr–Rh and Zr–Ir systems have some differences in the topology of the phase diagrams in the range of existence of the equiatomic phases. However, this should not affect the properties of the alloys, with the transformation $\text{B2} \rightleftarrows \text{B19}'$ being common to both compounds.

The electrical resistivity analysis results for both the ZrRh and ZrIr phases in the temperature range 200–1100 °C presented in Fig. 5 demonstrate the occurrence of the transformation. The ZrRh and ZrIr

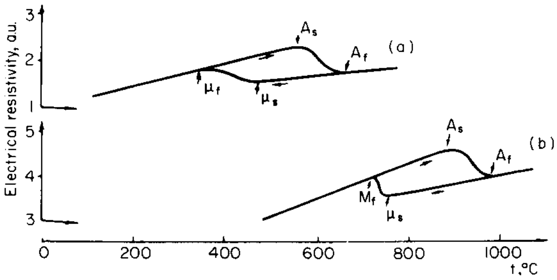

Fig. 5. Resistivity–temperature variation in ZrRh (a) and ZrIr (b) alloys.

electrical resistance polytherms are similar. The transformation temperatures determined from these curves are $M_S = 480$ °C, $M_f = 350$ °C, $A_S = 570$ °C and $A_f = 680$ °C for ZrRh and $M_S = 740$ °C, $M_f = 710$ °C, $A_S = 880$ °C and $A_f = 940$ °C for ZrIr, which are in good agreement with the data obtained from the thermal analysis measurements. Repeated cycles of "heating–cooling" in the transformation range do not result in changes in the critical temperatures. The temperature hysteresis in both cases is above 200 °C.

Thus it has been determined unequivocally that the ZrRh and ZrIr CsCl-type equiatomic compounds undergo a structural phase transformation on cooling according to the scheme $B2 \rightleftarrows B19'$, with a transformation hysteresis width of about 200 °C. The ZrRh alloy has been tested thermomechanically to determine the existence of the shape memory effect (SME) caused by this structural phase transformation (Fig. 6). The specimen was $0.8 \times 2 \times 20$ mm^3 in size and the load was 400 gf. The full shape restoration of the specimen was observed in spite of the temperature hysteresis being greater than for the TiNi compound [8]. Full shape restoration took place also after more than 20 cycles of "heating–cooling". The critical transformation temperatures measured both by these tests and by the electrical resistivity method were the same. In view of the isostructurality of both the original ZrRh and ZrIr phases and their transformation products, the existence of the SME in the ZrIr compound can also be expected.

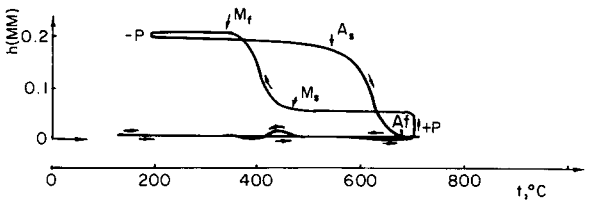

Fig. 6. ZrRh thermomechanical curve.

References

1 V.N. Yeremenko, E.L. Semenova, V.G. Choruzaja and T.D. Shtepa, in *Physical Chemistry of Inorganic Materials,* Vol. 1, Naukova Dumka, Kiev, 1988, p. 257.

2 A.E. Dwight, *Trans. Metall. Soc. AIME, 215* (1959) 283.

3 A. Raman and K. Schubert, *Z. Metallkd., 55* (1964) 704.

4 F.E. Wang, *J. Appl. Phys., 38* (1967) 822.

5 J.L. Jorda, T. Graf, L. Schellenberg, I. Muller, K. Cenzual, Y.C. Gachon and I. Hertz, *J. Less-Common Met., 136* (1988) 313.

6 V.N. Yeremenko, E.L. Semenova, T.D. Shtepa and Yu. V. Kudryavtsev, *Dopov. Akad. Nauk Ukr. RSR, Ser. A, 10* (1978) 943.

7 I.A. Arbuzova, Yu. N. Koval, V.V. Martynov and L.G. Chandros, *Fiz. Met. Metall., 35* (1973) 1278.

8 A.I. Lotkov and V.N. Grishkov, *Izv. Vyssh. Ucheb. Zav. Ser. Fiz., 27* (1985) 68.